Real-Time Kinetics of the Uptake of $ClONO_2$ on Ice and in the Presence of HCl in the Temperature Range 160 K ≤ *T* ≤ 200 K

R. Oppliger, A. Allanic, and M. J. Rossi*

Laboratoire de Pollution Atmosphérique et Sol, Département de Génie Rural, Ecole Polytechnique Fédérale de Lausanne, CH-1015 Lausanne, Switzerland

Received: May 9, 1996; In Final Form: December 20, 1996[⊗]

Pulsed dosing and steady state experiments of $ClONO_2$ on ice at 180 and 200 K studied in a low pressure flow reactor reveal a temperature-independent reactive uptake coefficient γ of 0.2 ± 0.05 at limiting doses and low flow rates of 10^{14} molecules per pulse and 10^{14} molecules s^{-1}, respectively. The reaction involves the formation of a precursor in a slow process releasing HOCl. This precursor does not interact with HCl. The reaction of $ClONO_2$ with HCl was studied under pulsed, concurrent, and sequential flow conditions and was found to follow a direct mechanism. The formation of Cl_2 occurs promptly on the time scale of several tens of milliseconds. The reactive uptake coefficient at equivalent flow rates of $ClONO_2$ and HCl was measured to be 0.14 ± 0.05 and 0.26 ± 0.05 at 200 and 180 K, respectively. At a 3-fold excess of HCl γ increases to 0.24 ± 0.05 and 0.34 ± 0.05 at 200 and 180 K, respectively. HOCl is found to interact with ice at $T > 173$ K and pressures of approximately 10^{-6} Torr only up to the extent of 5% of a monolayer beyond which it saturates. Arguments are put forward in favor of an ionic displacement mechanism in both reactions. The difference between the precursor mechanism of $ClONO_2$ interaction on ice and the direct interaction of $ClONO_2$ with HCl on ice may have ramifications for atmospheric chemistry which are briefly discussed.

1. Introduction

Heterogeneous processes in the stratosphere convert inactive chlorine in the form of reservoir molecules such as HCl and $ClONO_2$ during the polar night into an active photolyzable form such as HOCl and Cl_2 on the surfaces of tiny frozen atmospheric particulates called polar stratospheric clouds (PSC's) according to the following reactions:[1]

$$ClONO_2 + H_2O \rightarrow HOCl + HNO_3 \quad (1)$$

$$ClONO_2 + HCl \rightarrow Cl_2 + HNO_3 \quad (2)$$

$$HOCl + HCl \rightarrow Cl_2 + H_2O \quad (3)$$

Cl_2 releases atomic chlorine upon photolysis. Hypochlorous acid (HOCl) is known to be an important temporary reservoir of atmospheric chlorine, releasing it through photolysis or chemical reaction.

These PSC particles act as catalytic surfaces in the ozone destruction cycle in which chlorine chemistry plays a dominant role.[2,3] So far there is only circumstantial evidence as to the true chemical composition of PSC's.[4] Nevertheless, two broad classes of stratospheric particles may be distinguished based on laboratory results. PSC's of type I are thought to consist of nitric acid trihydrate (NAT) laced with small albeit variable amounts of HCl and formed at temperatures lower than 188 K. PSC's of type II correspond to ice particles and are generated at temperatures lower than 183 K at a typical vapor pressure of 5 ppm.[5] In addition, sulfuric acid aerosol at various concentrations was held responsible for the loss of background stratospheric ozone due to heterogeneous hydrolysis reactions of reservoir molecules.[6] Recently, the identity of stratospheric particulate in terms of the classification scheme type I and II has come under scrutiny and laboratory observations are invoked to distinguish additional fluid supercooled particles of saturated ternary solutions of $H_2SO_4-HNO_3-H_2O$ containing traces of HCl.[6−8] In addition, there is evidence from satellite optical measurements that disputes the identity of PSC's in terms of the classical breakdown into type I and type II.[9] Whatever the exact composition of those stratospheric particles may be, it is clear that appropriate substrates always seem to exist to support heterogeneous processes regardless of altitude and water partial pressure.[10] The present study emphasizes ice as a substrate, addressing stratospheric processes at low temperatures in the neighborhood of 180 K as well as reactions on ice crystals occurring in high-altitude cirrus clouds or aircraft contrails in the upper troposphere.[11]

Most of the recent kinetic data of heterogeneous reactions of chlorine nitrate, $ClONO_2$, on ice with and without HCl have been obtained by flow tube measurements. The reactive gases are mixed with He as a carrier gas and are interacting with the ice-coated walls of the flow tube.[7,12−15] For reactions 1 and 2, the values of the reactive uptake coefficient γ of $ClONO_2$ are summarized in Table 1. Some authors have reached the conclusion that reaction 2 does not occur as written in view of the rapid reaction between HOCl and HCl at the interface. Instead, they propose a fast conversion of $ClONO_2$ to HOCl according to reaction 1 followed by the rapid reaction between HOCl and HCl following reaction 3. As will be shown later we surmise that at least for ice substrates the above proposal needs careful reexamination.

In this study, the uptake kinetics of the gas is followed in real time using time-dependent mass spectrometry (MS), thus providing an independent and complementary confirmation of the steady state results. It seemed important to validate the existing kinetic data which are used in modeling calculations of the stratosphere by using a very different experimental approach. In addition, it was our goal to study the interfacial processes 1, 2, and 3 from a mechanistic point of view in order to be able to extrapolate laboratory kinetic data to realistic atmospheric conditions.

* To whom correspondence should be addressed.
[⊗] Abstract published in *Advance ACS Abstracts,* February 15, 1997.

S1089-5639(96)03065-4 CCC: $14.00

TABLE 1: Uptake Coefficients (γ) of $ClONO_2$ and $ClONO_2$ + HCl on Ice

T (K)	γ	references
	(a) $ClONO_2$ on Ice	
191	0.8 (+0.2, −0.3)	Hanson and Ravishankara, 1992 (ref 12)
191	$(3.0 \pm 1.0) \times 10^{-1}$	Hanson and Ravishankara, 1993 (ref 13)
188	3.0×10^{-2}	Chu, Leu, and Keyser, 1993 (thin ice film)
188	1.3×10^{-1}	Chu, Leu, and Keyser, 1993 (thick ice film) (ref 14)
195	$(8.0 \pm 2.0) \times 10^{-2}$	Zhang, Jayne, and Molina, 1994 (ref 7)
180	$(2.0 \pm 0.5) \times 10^{-1}$	this work
200	$(2.0 \pm 0.5) \times 10^{-1}$	this work
	(b) $ClONO_2$ + HCl on Ice	
200	0.27 (+0.73, −0.13)	Leu, 1988 (ref 15)
191	0.3 (+0.7, −0.1)	Hanson and Ravishankara, 1992 (ref 12)
188	$(2.7 \pm 1.9) \times 10^{-1}$	Chu, Leu, and Keyser, 1993 (thick ice film) (ref 14)
180	$(2.6 \pm 0.5) \times 10^{-1}$	this work
200	$(1.4 \pm 0.5) \times 10^{-1}$	this work

TABLE 2: Characteristic Parameters of the Knudsen Cell Used in this Study[a]

orifice diameter (mm)	k_{esc} (s^{-1})	residence time (s)
1.0	$0.013(T/M)^{0.5}$	$76.5(M/T)^{0.5}$
4.0	$0.245(T/M)^{0.5}$	$4.04(M/T)^{0.5}$
8.0	$0.796(T/M)^{0.5}$	$1.23(M/T)^{0.5}$
14.0	$1.88(T/M)^{0.5}$	$0.528(M/T)^{0.5}$

[a] Volume = 1800 cm^3; reactive area = 17.0 cm^2; $\omega = 34.7(T/M)^{0.5}$ s^{-1}. [b] The gas number density n may be calculated by $n = F^{i}_{M}/(V \cdot k_{esc})$, with F^{i}_{M} being the flow rate of species M into the Knudsen cell.

2. Experimental Section

The uptake measurements were carried out in a low-pressure flow reactor whose design and operation has been described elsewhere.[16] Briefly, the uptake measurements are performed in a Knudsen reactor operated in the molecular flow regime in order to make the kinetics of the heterogeneous reaction devoid of limiting gas diffusion. The reactor has two compartments which can be separated by an O-ring sealed plunger to allow for isolation of the ice sample during reference experiments. The escape aperture and thus the residence time of the average molecule in the gas phase may be varied by fitting a plunger-mounted plate with orifices onto the permanent, that is, largest, aperture. Both a change of the diameter of the escape orifices and a change in the flow rate of the gas into the reactor over a range of almost 3 orders of magnitude (1.0×10^{14} to 5.0×10^{16} molecules s^{-1}) affords the necessary variation of pressure and lifetime required to study the mechanism of heterogeneous reactions. The reactor is equipped with two types of inlet ports, one of which is a needle valve for continuous flow operation and the other of which is a wide (1.5 cm diameter) port onto which a pulsed valve is mounted. The pulsed valve experiment is especially suited for kinetic studies as it amounts to the real-time measurement of the lifetime of a gas burst injected into the reactor in the presence of an active surface. The pulsed valve was supplied by General Valve (Series 9, 2 mm diameter orifice). Characteristic parameters of the Knudsen reactor used in this study are displayed in Table 2 together with the range of variation of the experimental variables.

Molecules escaping through a selected orifice form an effusive (thermal) molecular beam which is coaxially aligned and monitored using an electron-impact quadrupole mass spectrometer (Balzers QMG 421). Prior to ionization, the molecular beam is chopped by a 150 Hz tuning fork or variable-speed chopper wheel located in the lower of the two differentially pumped chambers. Phase-sensitive detection (PSD) of the modulated component of the ion current was performed using a lock-in amplifier (Stanford Research Systems SR 850). The PSD scheme was used to discriminate the reactant or product effusive molecular beam from the background within the stainless steel chamber housing the mass spectrometer (MS).

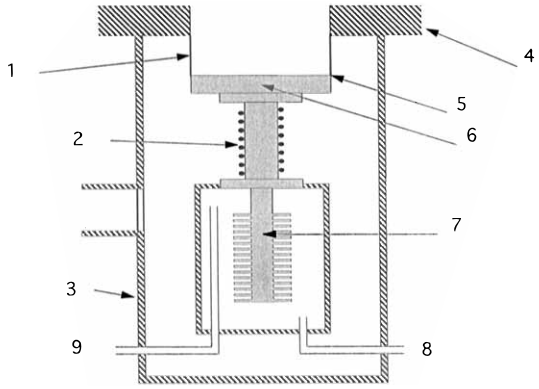

Figure 1. Schematic view of the low temperature support: 1, 0.3 mm thick stainless steel wall; 2, heating wires wound around copper core; 3, evacuated stainless steel jacket; 4, stainless steel flange; 5, welded steel−copper connection; 6, sample dish made out of copper; 7, copper core immersed into liquid nitrogen heat exchanger; 8, liquid nitrogen inlet; 9, liquid nitrogen outlet.

We used a low temperature support displayed in Figure 1 in order to attain and control temperatures in the range between 130 and 300 K. The ice sample is deposited from the gas phase on a wax-coated copper dish 6 forming the bottom of a cylinder with 0.3 mm thick stainless steel walls 1. A copper core is establishing mechanical contact with the copper dish (6) on the other side of the high vacuum with the heat exchanger 7. The temperature of the core is regulated by both heating and cooling processes. The heating cycle is achieved by a resistively heated electrical wire 2 wound around the copper core whereas the cooling cycle is achieved by passing cold dry air through tubes 8 and 9 coming from an aluminum coil immersed in liquid nitrogen and flowing into the heat exchanger (7). The temperature regulation consists of alternating periods of cooling and heating and is performed using a PID temperature controller. The internal volume of the support is evacuated in order to minimize the unwanted heat transfer of the room temperature walls 3 of the low temperature support to the temperature-controlled parts 5, 6, and 7 inside the low temperature support.

The ice samples were prepared by admitting a high H_2O flow rate of approximately 1×10^{19} molecules s^{-1} into the reactor once the sample dish had reached the temperature of the experiment. Exposure of this flow rate to the cold copper substrate for approximately 5 min resulted in a thick ice film of up to 2×10^5 monolayers which was kept in thermodynamic equilibrium by adjusting the external water flow so as to cancel evaporation and condensation rates, thus resulting in no net water vapor uptake. The temperature of the ice sample was verified by measuring the steady state water vapor pressure

which leads to a calculated equilibrium vapor pressure. The temperature agreed to within ±0.5 K with the nominal values of the vapor pressure.[17] We think that the kinetic results obtained on vapor phase deposited ice samples showed less of a scatter than the ones where liquid water was frozen to the required temperature but were identical in every other respect. We therefore exclusively report results obtained on vapor deposited ice samples.

2.1. Synthesis of Cl_2O. Dichlorine monoxide was synthesized from reacting Cl_2 with yellow HgO and subsequent distillation of the orange-brown Cl_2O at a temperature of approximately 195 K following standard procedure.[18]

2.2. Synthesis of HOCl. HOCl was synthesized by mixing Cl_2O and H_2O vapor in a vacuum line at room temperature. After a few minutes the trap was cooled down to 170 K and the excess Cl_2/Cl_2O was subsequently pumped away before HOCl was let into the reactor. We thus obtained a clean source of HOCl with the only contamination being Cl_2O and Cl_2 at low levels observed by mass spectrometry. Neither of these species interacted with the ice sample as determined from separate reference experiments.

2.3. Synthesis of $ClONO_2$. Chlorine nitrate was synthesized by reacting Cl_2O with excess N_2O_5 at low temperature according to the procedure described by Timonen et al.[19] rather than following the synthesis worked out by Schack.[20] After purification no impurities could be detected in the mass spectrum.

The synthesis of N_2O_5 closely follows the procedure published in ref 21 where NO_2 reacts with excess ozone to result in N_2O_5.

3. Results and Discussion

3.1. HOCl on Ice. In view of its importance for the subsequent discussion, we started our investigation with the characterization of the kinetic behavior of HOCl on ice. Hypochlorous acid (HOCl) is the primary product of reaction 1. Experiments were performed at different temperatures and continuous low flow rates on the order of 10^{14} molecules s^{-1} corresponding to a partial pressure of about 10^{-6} Torr in order to determine the uptake of HOCl on ice. These experiments did not reveal any uptake of HOCl. At temperatures below 173 K HOCl starts to condense at the used flow rates. The amount of HOCl condensed may be quantitatively recovered and subsequently recorded using MS at *m*/*e* 52 or 54 as it is desorbing from the interface with increasing substrate temperature. Pulsed valve experiments, however, clearly showed that there is an interaction at temperatures above 173 K for doses up to but not exceeding approximately 5% of a formal monolayer corresponding to a pulse of less than 5×10^{14} molecules. At higher doses HOCl does not show any interaction with ice due to apparent saturation of the ice. The weak interaction of HOCl with ice is in general agreement with experiments conducted in flow tube reactors.[2,12,23]

Moreover, when we monitored Cl_2O at *m*/*e* 86, its molecular ion peak, we never observed any change in MS signal. This indicates negligible heterogeneous interaction of Cl_2O with ice within our temperature range (160−200 K) and shows that the equilibrium 4 is not established on ice under our experimental conditions.

$$2HOCl \leftrightarrows Cl_2O + H_2O$$
$$\Delta H^\circ_r = -1.0 \text{ kcal/mol} \quad \text{(ref 22)} \quad (4)$$

In the presence of HCl, hypochlorous acid readily reacts to result in Cl_2 as a primary reaction product until the amount of HCl previously deposited on the surface has been quantitatively converted according to reaction 3. This experiment is performed in two steps. In the first, HCl is taken up by the ice sample in a rapid and efficient process leading to a quasi-liquid layer of HCl dissolved in H_2O.[23] The second step of the experiment consists of exposing a known flow of HOCl to the HCl-doped ice. Typical results are displayed in Figure 2, where we observe a sharp rise in the MS signal of Cl_2 monitored at *m*/*e* 70 (Cl_2^+) with a concomitant dip at *m*/*e* 52 ($HOCl^+$) indicating rapid conversion of HOCl to Cl_2 corresponding to $\gamma = 0.15$ for reaction 3. In addition, the strong signal at *m*/*e* 51 indicates a significant impurity of Cl_2O (10−50%) in the HOCl sample because the intensity of the fragment ClO^+ (*m*/*e* 51) in pure HOCl is only approximately 10% of the parent at *m*/*e* 52.[24] Thus, the dip in the signal at *m*/*e* 51 indicates that reaction 5 is occurring at similar rates because Cl_2O itself does not interact with ice at 200 K:

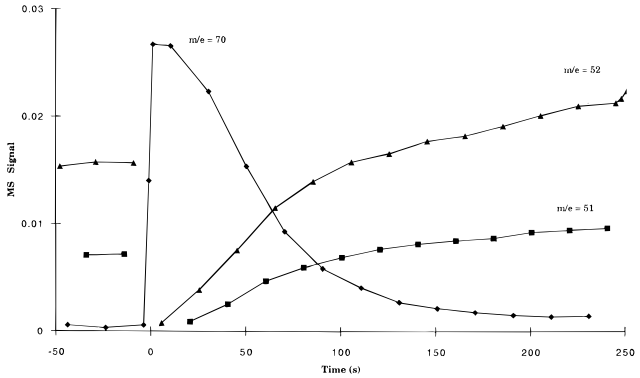

Figure 2. Continuous-flow experiment of HOCl on ice previously exposed to HCl at 200 K performed in a 4 mm diameter aperture Knudsen cell at a flow rate of 1×10^{15} molecules s^{-1}. The slow rise at *m*/*e* 52 (HOCl) and *m*/*e* 51 which is primarily due to the Cl_2O contribution from the source is attributed to the unstable nature of this source. At $t = 250$ s the ice is isolated from the HOCl flow, thus preventing further interaction with the ice.

$$Cl_2O + HCl \rightarrow Cl_2 + HOCl \quad (5)$$

The proof for the occurrence of reaction 5 is 2-fold: First, a condensate of Cl_2O on the bare copper substrate at 150 K leads to quantitative formation of Cl_2 when titrated with HCl. This shows that the reverse disproportionation of Cl(1+) and Cl(1−) such as in reaction 5 occurs both with the acid HOCl and with its anhydride. Second, the reaction of a mixture of HOCl and Cl_2O with HCl-doped ice leads to Cl_2 in the amount of the sum of HOCl and Cl_2O at conditions typical of Figure 2.

For the conditions of Figure 2 the ice was doped with a total HCl dose of $(1.4 \pm 0.2) \times 10^{17}$ molecules. The number of HOCl and Cl_2O molecules taken up by the HCl-doped ice was $(1.4 \pm 0.2) \times 10^{17}$ and $(0.4 \pm 0.07) \times 10^{17}$, respectively. The titration according to reactions 3 and 5 resulted in a total of $(1.7 \pm 0.25) \times 10^{17}$ molecules of Cl_2 recovered indicating a satisfactory mass balance based on total chlorine recovered. The mass balance was obtained using MS calibrations for the flows of HOCl, HCl, and Cl_2, establishing a relationship between the MS signal intensity and the measured flow rate of the respective species.[25] Figure 2 shows that the rate of formation of Cl_2 gradually decreases as the reservoir of HCl at the interface gets increasingly depleted. At the same time the HOCl signal reaches its original strength indicating the end of the loss process, reaction 3, at $t = 250$ s. This experiment shows that practically all the HCl deposited at the surface is readily available for reaction with HOCl vapor.[26]

The reaction in reverse order (reaction of HCl on ice onto which HOCl was previously condensed) yields similar results.

The ice surface is exposed to HOCl at a temperature of 160 K, at which Cl_2O is not condensed under the present conditions. The subsequent exposure of the HOCl condensate to HCl gives rise to a constant rate of formation of Cl_2 up to an amount corresponding to the quantity of HOCl condensed from the gas phase. For example, $(7.5 \pm 1.1) \times 10^{17}$ molecules of HOCl were deposited on ice at 160 K. After titration with excess HCl according to reaction 3, $(5.9 \pm 0.9) \times 10^{17}$ molecules of Cl_2 were obtained indicating a satisfactory mass balance. This shows that reaction 3 is rapid and goes to completion even at those low temperatures. Other authors also took note of similar efficiencies of reaction 3.[2,7,12]

Nitric acid is the other primary product of reaction 1 and is known to modify the ice surface through formation of stable nitric acid hydrates.[27] Preliminary HNO_3 deposition experiments on ice were carried out at 200 K, during which the water vapor signal at *m*/*e* 18 was monitored. Because of the excess of water due to the macroscopic nature of these ice samples, it appeared that the influence of HNO_3 on the H_2O signal was weak on the time scales of interest. Additional experiments were performed in which HNO_3 was codeposited together with HOCl in equal flows onto ice at 160 K. HOCl did not measurably interact with such HNO_3 hydrates. Another question is whether the presence of nitric acid will affect both the yield and the rate of reaction 3. On the one hand, the chlorine budget remained unaffected after titration with HCl; on the other hand, the rate of Cl_2 formation resulting from reaction 3 decreased as a consequence of the presence of HNO_3 hydrates at the interface. The uptake of HCl being unaffected by the presence of HNO_3, we therefore assert that the rate-limiting process leading to the formation of Cl_2 is slowed down by these hydrates.

We suggest HOCl to be present in its undissociated form during reaction 3 in view of its weak acidity (p*K* 4.7) because the interaction of HCl with ice almost certainly leads to a high acidity environment in the course of the titration reaction. This conclusion is supported by the fact that HOCl cocondensed with HNO_3 on ice at 160 K obtains results identical to the experiment in the absence of HNO_3.

3.2. $ClONO_2$ on Ice. Aware of the facile saturation of $ClONO_2$ uptake on ice,[14,28] we first carried out pulsed valve experiments in the course of which we monitored the time-dependent signal at *m*/*e* 46 as a marker for the flow of $ClONO_2$ leaving the reactor. The resulting decays were all single exponentials, and the decay rate constant k_{decay} was the sum of k_{esc} and k_{eff}, the heterogeneous rate constant of interest. Therefore k_{eff} was determined from $k_{eff} = k_{decay} - k_{esc}$. The reactive uptake coefficient γ is determined from the measured rate constant k_{eff} for the heterogeneous loss of $ClONO_2$ on ice divided by the calculated collision frequency ω of the average molecule with the ice surface given in Table 2. Despite rapid rates of $ClONO_2$ disappearance in the presence of ice, no HOCl was observed in the first 10 pulses or so. Figure 3 displays the results obtained from pulsed valve experiments in synoptic form as a function of residence time and for two temperatures, 180 and 200 K. These results show the absence of a significant temperature dependence of γ as well as its decrease with increasing dose or residence time. The pulsed valve experiments presented in Figure 3 are therefore subject to surface saturation at longer residence time. It was necessary to lower the dose to 10^{14} molecules/pulse (roughly 1% of a nominal molecular monolayer of $ClONO_2$ on top of the ice surface) in order to observe a constant value of γ for the first few pulses. They resulted in constant values for k_{decay} which were also the largest measured in a consecutive series of pulsed dosing experiments. For the case described in Figure 4, we measured $k_{1°pulse} = 13$ s^{-1} for a $k_{ref} = 1.4$ s^{-1} leading to $k_{eff} = 11.6$ s^{-1} and $\gamma = 0.19$. At higher doses (10^{15} molecules/pulse) the value for γ decreased, indicating that the rate of $ClONO_2$ uptake was already subject to partial saturation even for the first pulse. We found this fact quite surprising considering that the number of molecules lost to the surface during the first pulse represented only about 10% of a nominal monolayer, assuming a monolayer coverage of 5×10^{14} molecules cm^{-2} for $ClONO_2$. This confirms the extreme sensitivity of reaction 1 to saturation in agreement with literature results.[14,28]

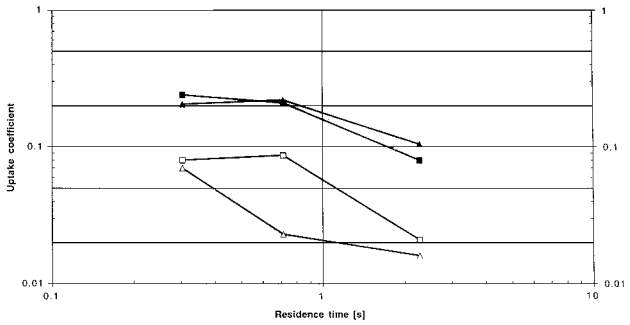

Figure 3. Summary of uptake coefficients (γ) of $ClONO_2$ on a fresh ice sample from pulsed valve experiments. Measurements at 180 K (squares) and 200 K (triangles) at a dose of 10^{14} (filled symbols) and 10^{15} molecules per pulse (open symbols). Each point corresponds to an experiment on a new ice sample because of rapid saturation of the ice upon $ClONO_2$ exposure.

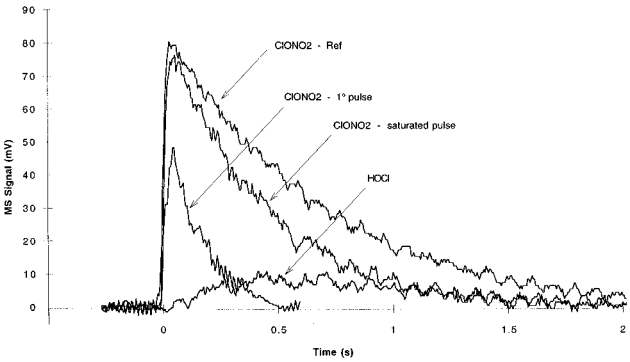

Figure 4. Pulsed dosing experiment of $ClONO_2$ on a surface saturated with $ClONO_2$ at 180 K performed in a 8 mm diameter aperture Knudsen cell. The curves "$ClONO_2$-Ref", "$ClONO_2$-1° pulse", and "$ClONO_2$-saturated pulse" correspond to the real-time decay of the MS signal at *m*/*e* 46 of the reference pulse in the absence of ice, the first reactive pulse, and a reactive pulse of $ClONO_2$ after saturation of the ice surface, respectively. The curve "HOCl" corresponds to the decay of the MS signal at *m*/*e* 52 in the presence of $ClONO_2$-saturated ice (see text for details).

After a series of several tens of pulses of $ClONO_2$ (depending on the dose) performed on an ice surface, HOCl begins to appear in the gas phase as is displayed in Figure 4. When a pulse of $ClONO_2$ interacts with such an ice surface which has been previously exposed to $ClONO_2$, a time-dependent rate of formation of HOCl is observed on the time scale of a few seconds, unlike the initial interaction of $ClONO_2$ with a fresh ice sample showing no HOCl at all. The resulting pulse of HOCl displayed in Figure 4 decays much more slowly than would correspond to k_{esc} ($k_{HOCl} = 0.6$ s^{-1} while the reference value corresponds to $k_{esc} = 2$ s^{-1} for HOCl). This indicates that the HOCl formation becomes rate limiting for $ClONO_2$ interaction with ice at 180 K. This observation seems to indicate the existence of a HOCl precursor at the surface which slowly releases HOCl into the gas phase.

We performed continuous flow experiments as well in order to confirm or reject the equivalence of the uptake coefficients

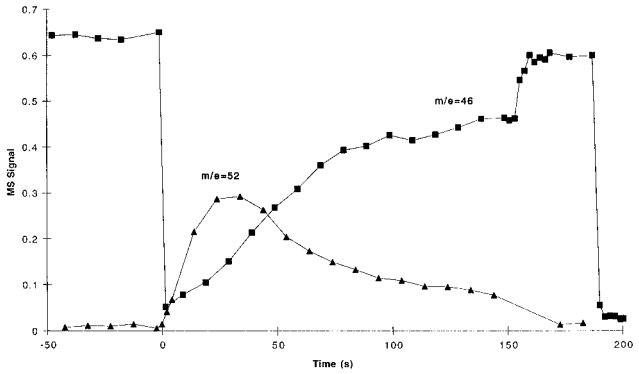

Figure 5. Typical continuous-flow experiment of $ClONO_2$ on ice at 180 K performed in a 4 mm diameter aperture Knudsen cell. $ClONO_2$ is let into the reactor at $F^{i}_{ClONO_2} = 1 \times 10^{14}$ molecules s^{-1} and monitored at *m*/*e* 46. HOCl is monitored at *m*/*e* 52.

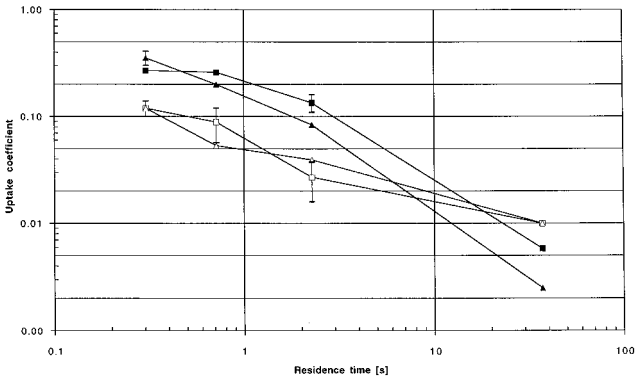

Figure 6. Summary of initial uptake coefficients (γ_0) of $ClONO_2$ on ice from continuous-flow experiments. Measurements at 180 (squares) and 200 K (triangles) at a flow rate of 10^{14} (filled symbols) and 10^{15} molecules s^{-1} (open symbols).

from both types of experiments. The continuous flow experiments show a pronounced flow rate dependence of the initial uptake coefficient γ_0. The partial pressure of $ClONO_2$ at the corresponding flow rate $F^{i}_{ClONO_2}$ is given by $P_{ClONO_2} = F^{i}_{ClONO_2}(\tau/V)$, where V is the volume of the Knudsen cell and τ is the measured gas phase residence time equal to $1/k_{esc}$ (Table 2).

Figure 5 displays a typical steady state experiment, where an ice sample at 180 K is exposed to a constant low flow of $ClONO_2$ of 10^{14} molecules s^{-1} monitored at *m*/*e* 46 (NO_2^+). Upon exposure of the ice sample, the MS signal at *m*/*e* 46 rapidly drops corresponding to an initial value γ_0 equal to 0.3 for the rate of $ClONO_2$ uptake by ice. Subsequently, the signal at *m*/*e* 46 gradually rises again due to a rapid saturation process on ice and eventually tends toward a steady state level. The rate of formation of HOCl monitored at *m*/*e* 52 ($HOCl^+$) is slowly rising, reaching a steady state level similar to the $ClONO_2$ signal. It appears thus that both the rate of uptake of $ClONO_2$ and the rate of formation of HOCl are approaching steady state. At higher flow rates of $ClONO_2$ the adsorption behavior on ice becomes increasingly complex. Under these conditions Cl_2O is observed, which is thought to be the result of secondary reactions. Figure 6 presents a summary on the dependence of γ for reaction 1 as a function of residence time for the continuous flow experiments.

Table 3 summarizes the pulsed valve (PV) and the continuous flow (SS) experiments at low dose and low flow rate conditions. Both types of experiments confirm the absence of a significant temperature dependence of γ_0 and agree on a value of 0.2 ± 0.05. They underline again the extreme sensitivity of the ice surface to saturation by $ClONO_2$, especially when considering the precipitous drop of γ_0 in going from $\tau = 0.7$ to 2.3 s (Figure 6).

TABLE 3: Initial Uptake Coefficients γ_0 for $ClONO_2$ on Ice Resulting from Pulsed Valve (PV) and Continuous-Flow (SS) Experiments at 180 and 200 K at a Limiting Low Dose of 10^{14} molecules per pulse Corresponding to 1% of a Nominal Monolayer of $ClONO_2$ on Ice and Limiting Low Flow Rates on the Order of 10^{14} molecules s^{-1}

	PV		SS	
residence time (s)	180 K	200 K	180 K	200 K
2.3	8.00×10^{-2}	0.105	0.135	0.084
0.7	0.21	0.22	0.26	0.2
0.3	0.24	0.205	0.27	0.355

TABLE 4: Mass Balance (molecules) for Continuous-Flow Experiments of $ClONO_2$ of 10^{15} molecules s^{-1} at Three Temperatures and Gas Phase Residence Times[a]

	160 K	180 K	200 K
	Residence Time = 0.7 s		
r	0.33	0.90	1.00
uptake	$1.8 \times \times 10^{17}$	2.0×10^{17}	1.8×10^{17}
HOCl		1.8×10^{17}	1.8×10^{17}
Cl_2O	0.3×10^{17}		
Cl_2			
balance	0.3×10^{17}	1.8×10^{17}	1.8×10^{17}
	Residence Time = 2.3 s		
r	0.18	0.92	1.05
uptake	4.6×10^{17}	4.8×10^{17}	5.7×10^{17}
HOCl		2.4×10^{17}	6.0×10^{17}
Cl_2O	0.4×10^{17}	1.0×10^{17}	
Cl_2			
balance	0.8×10^{17}	4.4×10^{17}	6.0×10^{17}
	Residence Time = 37 s		
r	0.22	0.87	0.78
uptake	7.6×10^{17}	6.3×10^{17}	6.5×10^{17}
HOCl			2.5×10^{17}
Cl_2O	0.8×10^{17}	2.6×10^{17}	1.7×10^{17}
Cl_2	0.1×10^{17}	0.3×10^{17}	0.2×10^{17}
balance	1.7×10^{17}	5.5×10^{17}	5.1×10^{17}

[a] The uptake is based on the rate of disappearance of $ClONO_2$ at steady state conditions. The balance is the sum of the corresponding flows F°_{M} leaving the Knudsen cell ($=F^{\circ}_{HOCl} + 2F^{\circ}_{Cl_2O} + F^{\circ}_{Cl_2}$). The term $F^{\circ}_{Cl_2}$ was determined by titration with excess HCl after $ClONO_2$ exposure to ice (see text). The ratio *r* is given by the ratio of flows balance/uptake.

In a typical continuous flow experiment such as the one displayed in Figure 5, the mass balance reveals missing chlorine: the rate of uptake of $ClONO_2$ is larger than the rate of formation of HOCl. This corroborates our previous observations based on pulsed valve experiments that a precursor form for HOCl must exist at the ice interface. We obtained additional results from continuous flow experiments varying both the temperature of the ice and the residence time of the $ClONO_2$ molecules in the reactor. Our aim was to assess the influence of those parameters on the mass balance. The results are summarized in Table 4.

The results may be summarized as follows: (a) At a given residence time, increasing temperatures seem to favor the HOCl release from the precursor locked in the ice matrix, thus reflecting the increasing rate of thermal decomposition of the HOCl precursor. (b) The value of *r* measuring the ratio of the Cl(1+) flows (HOCl, $ClONO_2$, Cl_2O) leaving the Knudsen cell to the rate of $ClONO_2$ uptake on ice decreases with temperature, thus indicating the increasing importance of the chlorine (1+) reservoir at low temperature. The chlorine mass balance (*r*) seems satisfactory for ice at 200 and 180 K, whereas it is deficient at 160 K. In order to close the mass balance at 160

K, we "interrogated" the ice previously exposed to $ClONO_2$ by a HCl flow. We expected to titrate either the condensed HOCl or adsorbed $ClONO_2$ according to reactions 3 and 2, respectively. Much to our surprise it appeared that HCl was unable to convert the missing Cl(1+) species into Cl_2. This strongly suggests that the HOCl precursor is unreactive toward HCl.

However, the mass balance may be closed if the ice sample previously exposed to $ClONO_2$ is warmed up. The missing chlorine is quantitatively recovered and accounted for as HOCl desorbing into the gas phase and subsequently recorded using MS at *m*/*e* 52. This may indicate that the thermally unstable HOCl precursor must store HOCl in a molecular structure that is very similar to the one in the gas phase.

Our experimental technique only allows us to examine the gas phase and provides us with little or no information about the nature of the ice sample except for the measurement of the vapor pressure. Nevertheless, studies conducted on the interaction of $ClONO_2$ on alkali-metal halide salts showed that this molecule displayed a pronounced "sticky" behavior and that its uptake coefficient was unaffected by structural parameters such as the BET surface area.[29] This means that $ClONO_2$ only interacts with the external surface regardless of microstructural details of the surface such as the presence of pores. We therefore assert that our results are also valid on ice whatever its nature may be because we assume that the surface residence time of $ClONO_2$ on ice may be similar to the ones for alkali-metal halide salts.

3.3. $ClONO_2$ + HCl on Ice. *A. Sequential Flow of $ClONO_2$ and HCl on Ice.* The second series of experiments relating to reaction 2 consisted in sequential exposure of either component, namely HCl and $ClONO_2$ to the ice sample. We began this series by exposing the ice sample to a high flow rate of HCl for a given time so that several tens of nominal monolayers of HCl were deposited on the ice. The vapor pressure of HCl over the quasi-liquid layer of concentrated HCl solution on the ice agreed with theory from the phase diagram of the system HCl/H_2O.[23]

Figure 7 presents raw data of pulsed $ClONO_2$ experiments which were conducted on ice surfaces that had taken up a known amount of HCl. Figure 7a displays the significant decrease of the $ClONO_2$ pulse lifetime in the presence of a HCl-doped ice surface when *m*/*e* 46 is monitored as a function of time (pulse 1) compared to a reference pulse in the absence of HCl and ice. Without refreshing the HCl supply in between $ClONO_2$ pulses, the lifetime $1/k_{decay}$ of the second $ClONO_2$ pulse is already significantly longer because the rate of reaction 2 is decreasing due to the waning supply of HCl at the interface. The identical behavior may be observed when the product pulse Cl_2 is observed at *m*/*e* 70 as a function of time. The decisive advantage of pulsed experiments in mechanistic studies may be appreciated, using as an example reaction 2 where the rise of the product pulse of Cl_2 may be monitored in real time as shown in Figure 7b. From the prompt rise of *m*/*e* 70 upon pulsed exposure of $ClONO_2$ to ice, we may conclude that the mechanism of molecular chlorine formation is direct and therefore significantly different from the one for HOCl formation, taking place on a longer time scale (Figure 5). It is useful to remind the reader that prompt HOCl formation has never been observed in a pulsed experiment in which $ClONO_2$ was exposed to a fresh ice sample. This is consistent with the fact that reaction 1 involves a precursor which is stable on the time scale of the pulsed experiment. Moreover, we observe a decrease in the yield of Cl_2 upon repetitive exposure of $ClONO_2$ to the same HCl-doped ice sample, indicating a decreasing rate of formation of Cl_2 due to depletion of HCl at the ice interface

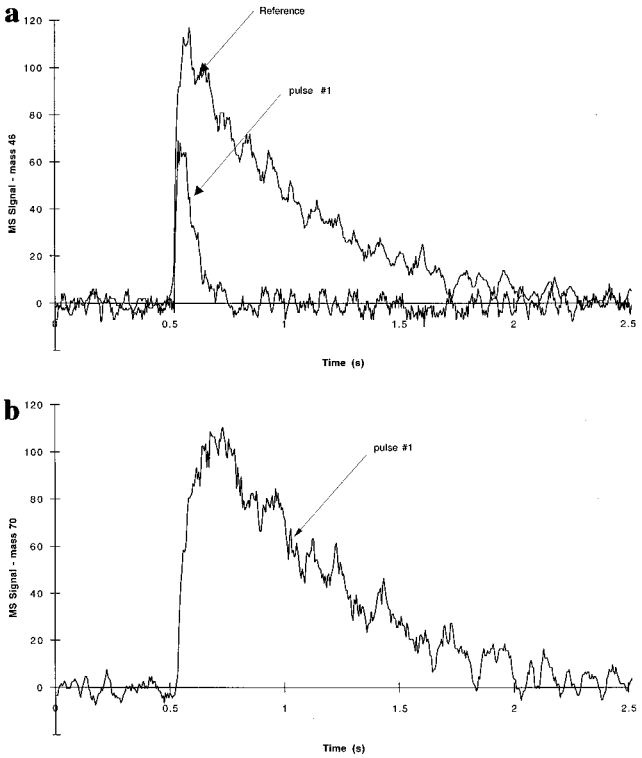

Figure 7. Pulsed dosing experiment of $ClONO_2$ uptake on ice previously exposed to HCl at 200 K performed in a 8 mm diameter aperture Knudsen cell. The $ClONO_2$ dose corresponds to 10^{14} molecules, equivalent to 1% of a formal monolayer. (a) $ClONO_2$ pulse monitored at *m*/*e* 46 in real time. The reference pulse was obtained from pulsed $ClONO_2$ dosing in the absence of ice; pulse 1 corresponded to the same dose in the presence of ice. (b) Cl_2 product pulse monitored at *m*/*e* 70 in real time in the presence of ice previously exposed to HCl.

TABLE 5: $ClONO_2$ Initial Uptake Coefficients γ_0 on HCl-Doped Ice for Continuous-Flow Experiments of $F^{i}_{ClONO_2} = 10^{15}$ molecules s^{-1} at 180 and 200 K and Two Gas Phase Residence Times

	γ_0	
residence time (s)	180 K	200 K
2.3	0.7 (+0.3, −0.5)	0.14 ± 0.13
0.7	0.64 ± 0.07	0.27 ± 0.07

even though there are more than stoichiometric amounts left on the ice. The decay of the MS signal at *m*/*e* 70 shown in Figure 7b corresponds to k_{esc} for Cl_2, indicating negligible interaction of chlorine with ice as expected.

The amount of $ClONO_2$ taken up by the ice surface is calculated by the difference between the calibrated integral of the reference pulse minus the integral of the reactant pulse. The mass balance between this amount (Figure 7a) and the yield of Cl_2 (Figure 7b) is closed at excess HCl. This indicates a 1:1 correspondence between reactant lost and product formed. In a typical experiment, the amount of $ClONO_2$ taken up by the surface is 1.5×10^{15} molecules and the amount of Cl_2 produced is 1.3×10^{15} molecules. This quantitative formation of Cl_2 within the error limits on a single pulse basis is thus an additional hallmark of reaction 2, emphasizing its efficiency and pointing toward a direct mechanism without the incidence of a precursor.

In addition, continuous-flow experiments were performed at different temperatures and gas phase residence times. The $ClONO_2$ uptake coefficients on HCl-doped ice are summarized in Table 5. We observe a negative temperature dependence of γ_0 which may be attributed to the fact HCl is possibly the

limiting reagent. HCl solubility in the H_2O/ice system decreases with temperature.[23]

For these continuous-flow experiments, molecular chlorine is the sole product detected at the beginning of the reaction. At the point where the supply of HCl at the interface becomes roughly equal to the quantity of $ClONO_2$ taken up, the observed rate of uptake of $ClONO_2$ begins to decrease and HOCl is beginning to appear. The Cl_2 signal drops to a low and constant level due to the small chlorine impurity in $ClONO_2$ and the HOCl slowly tends toward a steady state value which is proportional to the rate of uptake of $ClONO_2$. These results are consistent with the ones presented in the literature.[30] Of note is the fact that the HOCl signal still continues to increase after the rate of $ClONO_2$ uptake has reached steady state, indicating the slow release of HOCl from its precursor, probably by unimolecular decomposition.

The sequential exposure of $ClONO_2$ and HCl on ice in reverse order (HCl interaction with ice previously exposed to $ClONO_2$) has been discussed in section 3.2. It corresponds to our attempts to titrate HOCl at the interface using HCl. The results are displayed in Table 4. They reveal vanishing yields of Cl_2 indicating the kinetic stability of the HOCl precursor toward attack by HCl according to reaction 3. The mechanistic implications of this finding are discussed in more detail below.

B. Concurrent Flows of $ClONO_2$ and HCl. Reaction 2 was studied under simultaneous flow conditions similar to the flow tube experiments. We expected H_2O (ice) and HCl to compete for $ClONO_2$ which necessitated the monitoring of both reactants as well as the two possible products. In fact, both products are observed when $F^{i}_{HCl} \ll F^{i}_{ClONO_2}$. When F^{i}_{HCl} is turned off, the HOCl rate of formation slightly increases whereas the rate of uptake of $ClONO_2$ slightly decreases indicating a lower value of γ_0 for reaction 1 (Table 3) compared to γ_0 for reaction 2 (Table 5). Under conditions where $F^{i}_{HCl} = F^{i}_{ClONO_2}$ only Cl_2 is observed at the expense of HOCl, indicating the efficiency of reaction 2 over that of reaction 1. This fact is also underlined by the increased rate of uptake of $ClONO_2$ in the presence of HCl and the absence of any saturation under conditions of a sufficient continuous flow of HCl. Reaction 1 cannot compete with reaction 2 once stoichiometric quantities of HCl are adsorbed at the interface. While Cl_2 is always present as a product in a quantity equal to that of the minority species entering the reactor, HOCl is only generated when there is insufficient HCl to titrate $ClONO_2$ according to reaction 2. Moreover, the rate of appearance of HOCl in the gas phase is slow and follows the decrease of the reactive uptake of $ClONO_2$ due to saturation (Figure 5). On the other hand, the production of Cl_2 is immediate and remains constant throughout the experiment for the condition $F^{i}_{HCl} > F^{i}_{ClONO_2}$, speaking again for a direct interfacial reaction between HCl and $ClONO_2$ rather than for a process involving a HOCl precursor species.

Figure 8 displays the dependence of γ for reaction 2 as a function of F^{i}_{HCl}. In a series of experiments performed at 180 and 200 K in the 8 mm diameter aperture reactor and at a fixed flow of $ClONO_2$ of 10^{15} molecules s^{-1} we varied the flow of HCl between 2×10^{14} and 3×10^{15} molecules s^{-1}, the latter corresponding to 3 times the equivalent flow of $ClONO_2$. For the condition $F^{i}_{HCl} = 2 \times 10^{14}$ molecules s^{-1}, γ_0 of $ClONO_2$ lies between 4×10^{-2} at 200 K and 0.16 at 180 K. These values are similar to the ones found under similar flow conditions ($F^{i}_{ClONO_2} = 10^{15}$ molecules s^{-1}) for reaction 1 on ice for the same residence time of 0.7 s in the absence of HCl. These values of γ_0 are displayed in Figure 8 at $F^{i}_{HCl} = 0$. With increasing F^{i}_{HCl}, γ_0 gradually increases to reach a limiting value larger by up to a factor of 5 for the condition $F^{i}_{HCl} = 3F^{i}_{ClONO_2}$.

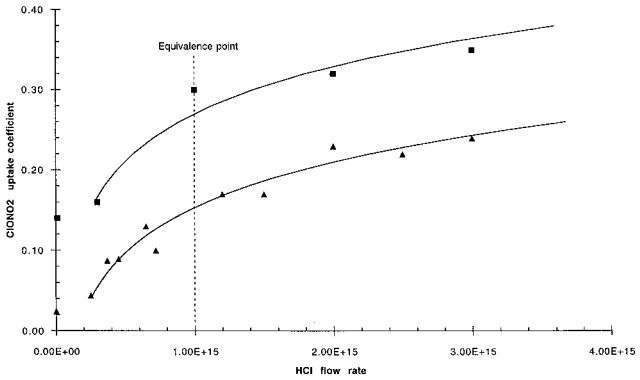

Figure 8. Dependence of the reactive uptake coefficients for concurrent flows of $ClONO_2$ and HCl on ice at 180 K as a function of F^{i}_{HCl} at constant $F^{i}_{ClONO_2} = 1 \times 10^{15}$ molecules s^{-1}. Measurements were performed at 180 (squares) and 200 K (triangles) using a 8 mm diameter aperture Knudsen cell.

This limiting value is close to the one found in the study of the sequential interaction of $ClONO_2$ on HCl-doped ice discussed above and presented in Table 5. This acceleration of the uptake kinetics upon increasing F^{i}_{HCl} reflects the larger efficiency and rate of reaction 2 with respect to reaction 1. An interesting result is the value of γ_0 at the equivalence point which is significantly smaller than the limiting value at the condition $F^{i}_{HCl} = 3F^{i}_{ClONO_2}$, even though HOCl cannot be detected anymore. The kinetics is thus a more sensitive probe of the state of the interface as the mere detection of reaction products. The temperature dependence of γ_0 at various stoichiometric ratios of HCl and $ClONO_2$ may reflect the temperature dependence of reaction 2 as discussed above and presented in Table 5.

4. Mechanistic Considerations

We now will attempt a molecular interpretation of the uptake of $ClONO_2$ on ice using the results of both pulsed and continuous experiments. The disparate rate of fast disappearance of $ClONO_2$ interacting with ice and the slow rate of appearance of HOCl in pulsed valve experiments may be reconciled with the presence of a precursor of HOCl releasing it in a slow rate-controlling process. The existence of this precursor P is ascertained by the following observations:

(i) While HOCl has been shown to be marginally reactive on ice when produced via reaction 1, it seems to be formed in a slow rate-limiting step compared to $ClONO_2$ deposition as represented by pulsed valve (Figure 4) and continuous flow experiments (Figure 5).

(ii) HOCl only begins to appear in the gas phase after a series of several pulses indicating the accumulation of a precursor species on the surface (Figure 4). This is also corroborated by the slow appearance of HOCl in continuous-flow experiments (Figure 5) as well as by the deficiencies in the mass balance measured in continuous-flow experiments (Table 4).

(iii) The titration of this precursor by HCl is not observable on our time scale and may be thus inefficient, whereas condensed HOCl reacts promptly with HCl at 160 K (reaction 3), even in the presence of HNO_3. By warming up the ice sample, this precursor decomposes, and the observed HOCl closes the mass balance.

Sodeau and co-workers[31] identified a HOCl precursor species resulting from $ClONO_2$ interaction with ice using grazing incidence FTIR absorption and attributed it to the following process:[31,32]

$$ClONO_2 + H_2O \rightarrow H_2OCl^+ \cdots NO_3^- \qquad (6)$$

The precursor $H_2OCl^+\cdots NO_3^-$ (P) corresponds to a complex between protonated hypochlorous acid stabilized by nitrate ion and apparently does not form when HOCl interacts with HNO_3-containing ice, a fact that we also confirmed by the absence of any HOCl uptake on such surfaces. It apparently does not even form on concentrated sulfuric acid surfaces so that reaction 6 is the only means to generate protonated HOCl known to date. We assume that the HOCl precursor is identical to the one studied by Sodeau, even though the experimental conditions were significantly different. Their experiments were performed under conditions of excess $ClONO_2$, and it is possible that the structure and reactivity of the HOCl precursor under our conditions of a large excess of H_2O over $ClONO_2$ may be different from the one found by Sodeau et al.[32]

The driving force for the release of HOCl in the initial phase of the uptake reaction may be the exothermic formation of hydrated HNO_3 thus leading to the decomposition of P. Every molecule of HOCl evaporating from the ice interface liberates a molecule of HNO_3 which may form hydrates. After a finite amount of HNO_3 hydrates have been deposited, the uptake of $ClONO_2$ slows down even though the rate of formation of HOCl by thermal decomposition of P continues. Supporting evidence for this proposal comes from the fact that the uptake coefficient of $ClONO_2$ on NAT is significantly lower than on pure ice.[13,33] If the $ClONO_2$ flow is interrupted for several minutes after the system has converged to steady state, the adsorption rate does not change after continuation of the uptake experiment thus indicating that the composition of the interface remains stable.

HNO_3 is known to form thermodynamically stable hydrates in the present temperature and concentration regime, such as $HNO_3 \cdot 3H_2O$ (NAT) or $HNO_3 \cdot H_2O$ (NAM).[10,23,34] In the first stage of $ClONO_2$ adsorption on ice we observe the formation of an amorphous HNO_3 layer because the H_2O signal does not change from its initial value given by the ice partial pressure at the given temperature. When a nominal monolayer of HNO_3 resulting from $ClONO_2$ hydrolysis, reaction 1, has been deposited, we observe the H_2O signal to slowly drop to a lower partial pressure indicating the incipient formation of a stable crystalline hydrate, presumably NAT. This phase transformation from an amorphous to a crystalline phase is a gradual process and takes place as the surface is increasingly covered with HNO_3 which binds H_2O molecules in an exothermic process. This phase transformation has also been observed in flow tube experiments reported by Hanson.[27] If $ClONO_2$ adsorption is taking place on a surface that previously has taken up several monolayers of HNO_3 from the gas phase, the rate of $ClONO_2$ adsorption is markedly slower and leads to typical values of γ between 10^{-4} to 10^{-2}, a result that is consistent with literature values obtained from flow tube experiments.[6,7,13,33] This shows that the presence of HNO_3 hydrates at the interface has a marked effect on the rate of $ClONO_2$ uptake.

Another diagnostic experiment that further shows the key role played by the presence of HNO_3 on the ice surface involves adding a flow of NH_3 to the flow of $ClONO_2$ interacting with ice. In this case no saturation of the $ClONO_2$ uptake is observed, even at a high flow rate of $ClONO_2$. Halting the flow of NH_3 brings back the "normal" behavior and saturation immediately sets in when the flow of $ClONO_2$ continues. No HOCl is observed because it is neutralized to $NH_4^+ClO^-$; instead a large flow of Cl_2O is observed. Apparently the interaction of condensed phase ClO^- with $ClONO_2$ leads to Cl_2O, reaction 7. In a similar way HOCl interacting with ClO^- also leads to Cl_2O according to a S_N2-type nucleophilic displacement, reaction 8:

$$ClO^- + ClONO_2 \rightarrow Cl_2O + NO_3^- \quad (7)$$

$$ClO^- + HOCl \rightarrow Cl_2O + OH^- \quad (8)$$

The formation of Cl_2O seems to be a secondary product and primarily due to high flow rates of $ClONO_2$. This conclusion is valid for both pulsed valve and steady state experiments.

To our surprise, no Cl_2 was ever observed when we attempted to titrate P using HCl, analogous to the results noted by Sodeau and co-workers.[32] Apparently P is totally unreactive toward HCl whose uptake on ice previously exposed to $ClONO_2$ is unchanged with respect to the uptake on pure ice. Table 4 displays the product yields including those of Cl_2 after titration using HCl. It reveals that only at the highest pressure corresponding to the longest residence time and only at 160 K was a small Cl_2 yield ever observed which could stem from traces of HOCl adsorbed onto the ice. This observation falls far short of the expected quantitative conversion of Cl(1+) to Cl_2 which has been observed in flow tube studies of heterogeneous reactions of gas phase HOCl with HCl adsorbed on ice,[2,12,14] albeit under concurrent flow conditions.

When the titration was carried out in reverse order, that is by first exposing the ice to HCl and subsequently to $ClONO_2$, a quantitative yield of Cl_2 was obtained in a fast reaction until exhaustion of the original quantity of HCl taken up by ice. Both steady state and pulsed valve experiments emphasize the prompt rise of Cl_2 formed apparently in a direct reaction without the participation of a precursor. Figure 7b presents good evidence of rapid formation of Cl_2 occurring on the same time scale as the $ClONO_2$ interaction on ice, whereas HOCl has never been observed in a pulsed experiment at comparable doses. The titration reaction is apparently occurring in a S_N2-type fashion, reaction 9, where Cl^- is the nucleophile in the condensed phase generated by ionic dissociation of HCl and NO_3^- is the leaving group:

$$Cl^- + ClONO_2 \rightarrow Cl_2 + NO_3^- \quad (9)$$

When HCl and $ClONO_2$ are exposed to ice at concurrent flows, both HOCl and Cl_2 are observed when the HCl flow is below the equivalence point. Even though the primary product HOCl can no longer be observed at HCl flows exceeding the equivalence point, the $ClONO_2$ uptake coefficient still increases to reach a limiting value at approximately a 3-fold excess of HCl as displayed in Figure 8. Apparently both HCl and H_2O are competing for $ClONO_2$ at the interface with HCl winning the race in view of its higher reactivity (Table 5). Under those conditions P may never be generated in large quantities because $ClONO_2$ is consumed in the rapid reaction (9) or it may decay spontaneously thus releasing small amounts of HOCl which subsequently would react with HCl.[2,12,14] The negative temperature dependence of reaction 9 displayed in Figure 8 may be due entirely to the concentration increase of HCl in the HCl/ice system with decreasing temperature according to the phase diagram as it is apparently controlled by the availability of HCl at the interface. The temperature independence of reaction 1 displayed in Figures 3 and 6 attests to the temperature independence of the ionic displacement mechanism, a fact that has repeatedly been pointed out by others.[31,32,35]

5. Conclusions and Atmospheric Significance

The present experiments stress the real-time aspect of the measurements and agree very well with the continuous-flow experiments performed using the Knudsen cell (present work) and laminar flow tube experiments. Low dose experiments

involving nominal surface coverages in the percent range were performed so as to approach low densities of interest to atmospheric applications and to avoid saturation phenomena. In addition, extensive use of mass balance considerations have been used in order to better quantify the reaction kinetics. In summary, we would like to point out three major conclusions from this work:

1. HOCl does not interact with ice down to temperatures of 173 K up to pressures of 20 mTorr.

2. The heterogeneous reactions $ClONO_2 + H_2O$ and $ClONO_2 + HCl$ on ice occur by two different reaction mechanisms. The former involves a precursor corresponding to a complex between protonated HOCl and nitrate anion resulting in delayed formation of HOCl, whereas the latter involves a direct interfacial reaction leading to prompt formation of Cl_2 according to a nucleophilic displacement by Cl^-.

3. A conclusion of potential importance to atmospheric reactions is that the interaction of $ClONO_2$ with HCl on ice does not involve the intermediate formation of HOCl followed by the rapid reaction between HOCl + HCl resulting in Cl_2.

We may state a potentially important consequence of our work. For one, the sequence of exposure of HCl and $ClONO_2$ to ice may be important in the atmosphere because they are not equivalent with respect to Cl_2 formation. It seems however, that at small doses of $ClONO_2$ compatible with stratospheric densities HOCl may partly be released into the gas phase and partly stored in the condensed phase as P. Furthermore, the suggested liquid nature of stratospheric aerosols[8] may render the titration reaction more efficient if the saturated ternary solutions contain small amounts of HCl because of the expected instability of P in the fluid medium.

Acknowledgment. This work was funded by Grants 20-37599.93 and 20-43353.95 of the Swiss National Science Foundation (Fonds National Suisse) and by a contract administered by OFES to participate in the EU Environment Program "CABRIS" (*C*hlorine and *B*romine *R*eservoirs in the *S*tratosphere). Our thanks go also to Professor H. van den Bergh for his support and encouragement as well as his lively interest.

References and Notes

(1) Solomon, S.; Garcia, R. R.; Rowland, F. S.; Wuebbles, D. J. *Nature* **1986**, *321*, 755. Cicerone, R. J. *Science* **1987**, *237*, 35. Solomon, S. *Rev. Geophys*. **1988**, *26*, 131. World Meteorological Organization (WMO). *Scientific Assessment of Stratospheric Ozone: 1989*; Report No. 20; WMO: Geneva, 1990.

(2) Abbatt, J. P. D.; Molina, M. J. *Geophys. Res. Lett.* **1992**, *19*, 461.

(3) Wayne, R. P.; et al. *Halogen Oxides: radicals, sources and reservoirs in the laboratory and in the atmosphere*; European Commission, Air Pollution Research Report 55; European Commission, DG XII: B-1049 Brussels, 1995. Daniel, J. S. *J. Geophys. Res*. **1995**, *100*, 1271.

(4) Drdla, K.; Tabazadeh, A.; Turco, R. P.; Jacobson, M. J.; Dye, J. E.; Twohy, C.; Baumgardner, D. *Geophys. Res. Lett*. **1994**, *21*, 2475. Carslaw, K. S.; Luo, B. P.; Clegg, S. L.; Peter, Th.; Brimblecombe, P.; Crutzen, P. J. *Geophys. Res. Lett.* **1994**, *21*, 2479.

(5) Turco, R. P.; Toon, O. B.; Hamill, P. *J. Geophys. Res.* **1989**, *94*, 16493.

(6) Turco, R. P.; Whitten, R. C.; Toon, O. B. *Rev. Geophys*. **1982**, *20*, 233. Zhang, R.; Wooldridge, P. W.; Molina, M. J. *J. Phys. Chem*. **1993**, *97*, 8541. Beyer, K. D.; Seago, S. W.; Chang, H. Y.; Molina, M. J. *Geophys. Res. Lett.* **1994**, *21*, 871.

(7) Zhang, R.; Jayne, J. T.; Molina, M. J. *J. Phys. Chem.* **1994**, *98*, 867.

(8) Mackenzie, A. R.; Tolbert, M. A. *Nature* **1995**, *375*, 218. Tolbert, M. A. *Science* **1996**, *272*, 1597.

(9) Toon, B.; Vesala, T. *J. Geophys. Res.* **1995**, *100*, 11275.

(10) Wooldridge, P. J.; Zhang, R.; Molina, M. J. *J. Geophys. Res.* **1995**, *100*, 1389. Zhang, R.; Leu, M. T.; Keyser, L. F. *J. Phys. Chem.* **1994**, *98*, 13563.

(11) *AERONOX, The Impact of NO_x Emissions from Aircraft upon the Atmosphere at Flight Altitudes 8−15 km*; Schumann, U., Ed.; EC-DLR, Publication on Research related to Aeronautics and Environment, August 1995.

(12) Hanson, D. R.; Ravishankara, A. R. *J. Phys. Chem.* **1992**, *96*, 2682.

(13) Hanson, D. R.; Ravishankara, A. R. *J. Phys. Chem.* **1993**, *97*, 2802.

(14) Chu, L. T.; Leu, M.-T.; Keyser, L. F. *J. Phys. Chem.* **1993**, *97*, 12798.

(15) Leu, M.-T. *Geophys. Res. Lett.* **1988**, *15*, 17.

(16) Tabor, K. D.; Gutzwiller, L.; Rossi, M. J. *J. Phys. Chem.* **1994**, *98*, 6172.

(17) Marti, J.; Mauersberger, K. *Geophys. Res. Lett.* **1993**, *20*, 363.

(18) Knauth, H.-D.; Alberti, H.; Clausen, H. *J. Phys. Chem*. **1979**, *83*, 1604.

(19) Timonen, R. S.; Chu, L. T.; Leu, M.-T.; Keyser, L. F. *J. Phys. Chem*. **1994**, *98*, 9509.

(20) Schack, C. J. *Inorg. Chem.* **1967**, *6*, 1938.

(21) Fenter, F. F.; Caloz, F.; Rossi, M. J. *J. Phys. Chem*. **1996**, *100*, 1008.

(22) Wagman, D. D.; Evans, W. H.; Parker, V. B.; Schumm, R. H.; Halow, I.; Bailey, S. M.; Churney, K. L.; Nuttal, R. L. The NBS tables of chemical thermodynamic properties. *J. Phys. Chem. Ref. Data* **1982**, *11* (Suppl. 2).

(23) Molina, M. J. The Probable Stratospheric 'Ice' Clouds, Heterogeneous Chemistry of the 'Ozone Hole'. In *The Chemistry of the Atmosphere: Its Impact on Global Change*; Calvert, J. G., Ed.; IUPAC CHEMRAWN 1994; Blackwell Science Publishing: Oxford, U.K., 1994.

(24) Vogt, R.; Schindler, R. N. *Ber. Bunsen-Ges. Phys. Chem*. **1993**, *97*, 819.

(25) The mass spectrum of pure HOCl has been obtained by reacting dry $Ca(OCl)_2$ with HNO_3 inside the Knudsen cell.

(26) Abbatt, J. P. D.; Beyer, K. D.; Fucaloro, A. F.; McMahon, J. R.; Wooldridge, P. J.; Zhang, R.; Molina, R. *J. Geophys. Res*. **1992**, *97*, 15819. Flückiger, B.; Gutzwiller, L.; Thielmann, A.; Rossi, M. J. To be published.

(27) Hanson, D. *Geophys. Res. Lett*. **1992**, *19*, 2063.

(28) Hanson, D. R.; Ravishankara, A. R. *J. Geophys. Res.* **1991**, *96*, 5081. Leu, M. T.; Moore, S. B.; Keyser, L. F. *J. Geophys. Res*. **1991**, *95*, 7763.

(29) Caloz, F.; Fenter, F. F.; Rossi, M. J. *J. Phys. Chem*. **1996**, *100*, 7494.

(30) Hanson, D. R.; Ravishankara, A. R. *J. Phys. Chem.* **1994**, *98*, 5728.

(31) Sodeau, J. R.; Horn, A. B.; Banham, S. F.; Koch, Th. G. *J. Phys. Chem*. **1995**, *99*, 6258.

(32) Banham, S. F.; Horn, A. B.; Koch, Th. G.; Sodeau, J. R. *Faraday Discuss*. **1995**, *100*, 321.

(33) Hanson, D.; Ravishankara, A. R. *J. Geophys. Res*. **1993**, *98*, 22931.

(34) Worsnop, D. R.; Fox, L. E.; Zahniser, M. S.; Wofsy, St. C. *Science* **1993**, *259*, 71.

(35) Nelson, C. M.; Okumura, M. *J. Phys. Chem*. **1992**, *96*, 6112. Haas, B.-M.; Crellin, K. C.; Kuwata, K. T.; Okumura, M. *J. Phys. Chem.* **1994**, *98*, 6740. van Doren, J. M.; Viggiano, A. A.; Morris, R. A. *J. Am. Chem. Soc*. **1994**, *116*, 6957.